Genomic, Proteomic and Physiological Characterization of a T5-like Bacteriophage for Control of Shiga Toxin-Producing *Escherichia coli* O157:H7

Yan D. Niu[1], Kim Stanford[2], Andrew M. Kropinski[3,4], Hans-Wolfgang Ackermann[5], Roger P. Johnson[3], Yi-Min She[6], Rafiq Ahmed[7], Andre Villegas[3], Tim A. McAllister[1]*

1 Lethbridge Research Centre, Agriculture and Agri-Food Canada, Lethbridge, Alberta, Canada, 2 Alberta Agriculture and Rural Development, Agriculture Centre, Lethbridge, Alberta, Canada, 3 Public Health Agency of Canada, Laboratory for Foodborne Zoonoses, Guelph, Ontario, Canada, 4 Department of Cellular and Molecular Biology, University of Guelph, Guelph, Ontario, Canada, 5 Département de microbiologie, Faculté de médecine, Université Laval, Québec, Quebec, Canada, 6 Center for Vaccine Evaluation, Biologics and Genetic Therapies Directorate, Health Canada, Ottawa, Ontario, Canada, 7 Public Health Agency of Canada, National Microbiology Laboratory, Winnipeg, Manitoba, Canada

Abstract

Despite multiple control measures, *Escherichia coli* O157:H7 (STEC O157:H7) continues to be responsible for many food borne outbreaks in North America and elsewhere. Bacteriophage therapy may prove useful for controlling this pathogen in the host, their environment and food. Bacteriophage vB_EcoS_AKFV33 (AKFV33), a T5-like phage of *Siphoviridae* lysed common phage types of STEC O157:H7 and not non-O157 *E. coli*. Moreover, STEC O157:H7 isolated from the same feedlot pen from which the phage was obtained, were highly susceptible to AKFV33. Adsorption rate constant and burst size were estimated to be 9.31×10^{-9} ml/min and 350 PFU/infected cell, respectively. The genome of AKVF33 was 108,853 bp (38.95% G+C), containing 160 open reading frames (ORFs), 22 tRNA genes and 32 strong promoters recognized by host RNA polymerase. Of 12 ORFs without homologues to T5-like phages, 7 predicted novel proteins while others exhibited low identity ($<60\%$) to proteins in the National Centre for Biotechnology Information database. AKVF33 also lacked the L-shaped tail fiber protein typical of T5, but was predicted to have tail fibers comprised of 2 novel proteins with low identity (37–41%) to tail fibers of *E. coli* phage phiEco32 of *Podoviridae*, a putative side tail fiber protein of a prophage from *E. coli* IAI39 and a conserved domain protein of *E. coli* MS196-1. The receptor-binding tail protein (*pb5*) shared an overall identify of 29–72% to that of other T5-like phages, with no region coding for more than 6 amino acids in common. Proteomic analysis identified 4 structural proteins corresponding to the capsid, major tail, tail fiber and pore-forming tail tip (*pb2*). The genome of AKFV33 lacked regions coding for known virulence factors, integration-related proteins or antibiotic resistance determinants. Phage AKFV33 is a unique, highly lytic STEC O157:H7-specific T5-like phage that may have considerable potential as a pre- and post-harvest biocontrol agent.

Introduction

Shiga toxin-producing *Escherichia coli* O157:H7 (STEC O157:H7) continues to be one of the major pathogens responsible for foodborne infections in North America [1,2]. Although it has been nearly 30 years since STEC O157:H7 was first associated with disease in humans, frequent outbreaks as well as sporadic cases continue to occur, with a proportion of cases developing serious acute and chronic sequelae [3].

Healthy cattle are recognized as the primary reservoirs of STEC O157:H7 [4] and up to 30% of North American feedlot cattle shed these bacteria in their feces [4,5]. Fecal-contaminated meat, fruit, vegetables, and water are the most common infectious sources [3]. Consequently, the majority of mitigation practices developed to date have focused on preventing the adulteration of meat and other foods with STEC O157:H7 during slaughter, processing and retail handling [6]. Another complementary approach to reduce human infections is to mitigate STEC

O157:H7 on farm. However, few highly effective on-farm intervention strategies have been developed, although such technologies are being sought [6].

Bacteriophages (phages) are natural infectious agents of bacteria with either lytic or temperate life cycles. Interest in lytic phages as antimicrobial agents is increasing, owing to their target specificity, ability to self replicate and lyse bacteria, and ubiquity within the environment [7,8]. Phages are being reassessed for their ability to prevent and treat bacterial infections in humans [7], livestock [8,9] and plants [10] and to decontaminate processed foods and agricultural products [7,8]. Lytic phages have recently been shown to reduce populations of STEC O157:H7 *in vitro* [11,12] and within food matrices [13,14]. However, the complexity and abundant microflora of the ruminant gastro-intestinal tract pose a formidable challenge to the development of phage-based approaches to controlling STEC O157:H7 in ruminants [11,15]. Phages that specifically infect and kill a broad range of STEC

O157:H7 at low multiplicities of infection (MOI) in the intestinal tract or other environments are required mitigate this human pathogen.

Previously, we found that the presence of natural STEC O157:H7 phages in cattle and the environment are associated with a reduced prevalence of STEC O157:H7 [16]. Here we describe the genomic, proteomic and physiological characteristics of a STEC O157:H7-specific T5-like phage that was frequently isolated during our previous study. We hypothesized that this phage would have unique properties that would be conducive to the selection of phage that would be effective for pre- and post-slaughter control of STEC O157:H7.

Results

Phage structure, host range and physiological characteristics

Structurally, AKFV33 had an icosahedral head about 78 nm in diameter and a long (185×8.5 nm) rigid, non-contractile, striated tail that ended in a conical structure possessing terminal fibers (23×3 nm, Figure 1). In host range studies, phage AKFV33 was lytic for a wide range of STEC O157:H7 strains and did not lyse any of the non-O157 serotypes of *E. coli* strains examined (Table 1). Of 30 common phage types (PTs) of STEC O157:H7 strains, 27 representing 95% of Canadian STEC O157:H7 isolates (human and livestock) examined in 2007–2009 [2] were highly susceptible [12] to AKFV33 (Avg. MOI = 0.004 ± 0.01). Furthermore, all 27 STEC O157:H7 isolates from the feedlot of origin of AKFV33, five nalidixic acid-resistant strains of human and bovine origin as well as a reference strain EDL933 from a human were lysed by AKFV33 with extremely low MOIs ranging from 10^{-5} to 10^{-7}. The adsorption rate constant (k) was estimated to be about 9.31×10^{-9} ml/min (Figure 2). The one-step growth curve of AKFV33 propagated on STEC O157:H7 strain R508 in tryptic soy broth (TSB) medium revealed the latent and rise periods were approximately 29 and 14 min (Figure 2), respectively. The average burst size was estimated to be 350 plaque forming units (PFU)/ infected cell.
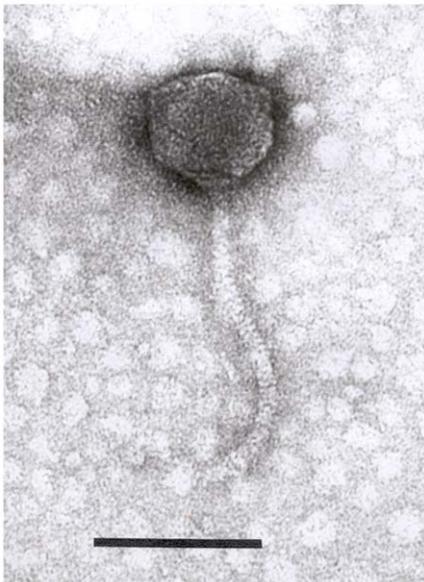
Figure 1. Transmission electron micrograph of AKFV33 negatively stained with uranyl acetate. Scale bar represents 100 nm.
doi:10.1371/journal.pone.0034585.g001

In acid tolerance studies, titers of phage AKFV33 dropped by 1.99 $\log_{10}$ PFU/ml (1.0% survival) after 15 min at pH 3.0 and were undetectable after 2 h, whereas after 16 h at pH 4.5 and 9.3, titres were reduced by 1.09 $\log_{10}$ (8.2% survival) and 0.12 $\log_{10}$ (76.3% survival) PFU/ml, respectively.

Genome description

The AKFV33 genome was ~111 kb and consisted of linear double-stranded DNA which was sequenced with ~300 fold coverage (Table 2). The three contigs which made up the total sequence were collapsed using PCR giving a final sequence of 108,853 bp (38.95% G+C). A total of 160 open reading frames (ORFs) and 22 tRNAs (Figure 3 and Figure S1; Table S1), which encoded for 18 amino acids were identified. Furthermore, 19 rho-dependent terminators and 32 promoters recognized by host RNA polymerase were identified. A consensus sequence of the promoters was TTGCTw (-35 box; where "w" = A or T) and TATAATA (-10 box) with a space of 17 to 18 bp between them (Figure S1). Regions of AT-richness were found upstream of -43 region (AAAAATT) and $+1$ region (TAAATT). Overall, codon usages of phage AKFV33 and STEC O157:H7 EDL933 were correlated (Pearson correlation coefficients $r = 0.51$, $P < 10^{-4}$, Figure S2).

In general, AKFV33 had a genome structure in common with T5-like phages including pre-early, early and late gene regions (Figure 3, Table S1). Position-specific iterated (PSI)-BLAST searches indicated that the protein products of 148 ORFs were similar to those of T5. Of the 12 ORFs without homology to T5 genes, 7 predicted completely novel proteins. None of the predicted proteins exhibited homology towards virulence factors, integration-related proteins or antibiotic resistance determinants. Comparative genomic analysis revealed that AKFV33 was collinear with 76–86% nucleotides similar to other members of the T5 group (Figure 4). Computational analysis of CoreGenes showed that AKFV33 shared 126 (75%), 133 (78.2%), 118 (82.5%), 136 (83.9%) and 132 (91%) homologues with phages T5 (GenBank accession #: AY587007), EPS7 (NC_010583), H8 (AC171169), T5 (NC_005859) and SPC35 (HQ406778), respectively.

Pre-early genes: The protein products of ORFs 1–16 encoded by pre-early genes in AKFV33 were conserved (Avg. 89% identity) with those of other T5-like phages. Only ORFs 3 and 14 were completely novel. ORFs 1, 4 and 6 encoded deoxynucleoside-5′-monophosphatase (92% identity), phage DNA transfer protein A1 (92% identity) and DNA-binding protein A2 (99% identity), respectively.

Early genes: One hundred nineteen ORFs produced proteins which theoretically function early in the phage infection cycle. The majority of these products (111 of 119) displayed an average identity of 89% with T5-like proteins, although 20 exhibited lower identity (38–79%). A high degree of similarity was found for those genes coding for products involved in DNA replication, repair, recombination, transcription, metabolism, cell lysis and signal transduction.

Eight ORFs were predicted to code for essential enzymes associated with nucleotide metabolism: thioredoxin (*nrdC*, ORF38), deoxynucleoside-5′-monosphate kinase (*dnk*, ORF44), thymidylate synthase (*td*, ORF93), dihydrofolate reductase (*frd*, ORF94), small subunit of aerobic ribonucleoside diphosphate reductase (*nrdB*, ORF95) and large subunit of aerobic ribonucleoside diphosphate reductase (*nrdA*, ORF97), anaerobic ribonucleoside triphosphate reductase (*nrdD*, ORF101) and deoxyuridine 5′-triphosphate nucleotidohydrolase (*dut*, ORF133). These eight ORFs exhibited an identity that was 95% of other T5-like phages.

Table 1. Host range and lytic capability of phage AKFV33.

Bacteria	Strains	No. of strains	Sensitivity[a] to AKFV33
STEC O157:H7	Reference strains		
	PTs[b] 1, 2, 4, 8, 10, 14, 14a, 21, 23, 24, 28, 31, 32, 33, 34, 38, 45, 46, 47, 48, 49, 50, 51, 54, 67, 68, 87	27	MOI = 0.004±0.01
	PTs 63, 70, 74	3	MOI = 3±0.4
	EDL933	1	MOI = 9×10^{-6}
	Nalidixic acid-resistant strains E32511 (PT4), CO281-31N (PT8), R508N (PT14), E318N (PT31), H4420N (PT87)	5	MOI = $(6 \pm 2) \times 10^{-6}$
	Endemic bovine isolates	27	MOI = $(7 \pm 3) \times 10^{-6}$
Non-O157 E. coli	ECOR collection[c] ATCC25922 (E. coli O6:K−)	73	No lysis observed

[a]Sensitivity is based on mean multiplicity of infection (MOI: the lowest ratio of phage to bacteria resulting in complete lysis of overnight bacterial culture within 5 h of incubation).
[b]PTs represents phage types of STEC O157:H7.
[c]ECOR collection represents standard reference strains of Escherichia coli [53].
doi:10.1371/journal.pone.0034585.t001

The replication cluster of AKFV33 was also highly-conserved (97% identity) compared to other T5-like phages, including components of the replisome; RNaseH (ORF90), DNA ligase (ORF119 and ORF120), DNA primase (ORF123), helicase (ORF122), DNA polymerase (ORF124), flap endonuclease (ORF132) and a replication origin binding protein (ORF112). Additionally, regions coding for two recombination enzymes D12 (ORF129) and D13 (ORF130) were both highly similar (92% identity) to those of other T5-like phages. However, genes (ORFs 96 and 111) coding for homing endonucleases (HEs) diverged from those reported for T5-like phages. The former, located between nrdA and nrdB, was 42% identical to H-N-H endonuclease of T5, while the latter had an identity that was only 32% identical to a protein of the *Pseudomonas* podovirus Φ2. ORFs 100 and 155 were predicted to code for a DNA-binding domain whereas ORF121 was predicted to code for a helix-turn-helix XRE domain that corresponded to a T5 phage DNA binding protein, D5 (95% identity).

Three protein products in the early-gene region encoded for a lysozyme (ORF41, 99% identity), holin (ORF42, 95% identity) and cell wall hydrolase SleB (ORF81, 83% identity). The AKFV33 holin, was predicted to be comparatively larger (24.7 kDa) and possess a single transmembrane domain as compared to the 2 to 3 domains that are typical of most phage holins [17].

Late genes: Tail component proteins (ORFs 135, 137–138, 145–146, 152 and pb2–5), head related proteins (ORFs 150 and 151), portal protein (ORF153) and terminase (ORF156) were identified in the ORFs 135 to 158. However, the late genes of AKFV33 were the least-conserved with an average identity of 82% as compared to other T5-like phages. Unlike the typical L-shaped tail fiber protein (Ltf) of T5, the tail fiber proteins of AKFV33 were predicted to be encoded for by two gene products associated with ORFs 135 (ltpB) and 137 (ltpA). Moreover, these two gene products exhibited low predicted identity (37–41%) to proteins in the tail fiber of *E. coli* phage phiEco32 of *Podoviridae* (ORF135), a conserved domain protein of *E. coli* MS196-1 (ORF137), and a putative side tail fiber protein of prophage from *E. coli* IAI39 (ORF137). To further elucidate this regions role in host-specificity, we generated GenBank flat files (*.gbk) extending from the flap endonuclease (D15) to the conserved hypothetical protein (ORF141) among T5-like phages and aligned them using a progressiveMAUVE algorithm (Figure S3). The results clearly showed that the sequence similarity declined markedly for genes encoding tail fibers from T5-like phages. The presence of ORF137

(Table 3 and Table S2; Figure 5, band C) was confirmed as the tail fiber protein by MALDI QqTOF Mass Spectrometry analysis. This gene product was also predicted to belong to the DUF1640 superfamily (cl06708) and with >0.6 probability contained two coiled-coil structures located from residues (249–276) and (314–346). As well, two coiled-coil structures (>0.6 probability) were found in ORF135 (residues 10–38 and 520–557). Similarly, ORF158 (pb5) encoded a receptor-binding tail protein of 585 amino acids, which is reputed to be responsible for binding to outer membrane proteins on the host surface during infection. In general, this protein shared only 29–72% identity to that of other T5-like phages (Figure S4). Furthermore, CLUSTALW showed that this receptor binding protein did not share more than 6 amino acids in common with other related T5-like phages (strains D1G, BF23 and ATCC11303-B5, Figure S4).

Proteomics

Mass Spectrometry identified four structural proteins with amino acid sequence coverage up to 57% (Table 3 and S2, Figure 5). The molecular mass of ORF167 (Figure 5, band B) was 51.7 kDa, being close to the predicted size of 50.5 kDa and in agreement with 51 kDa reported by Zweig and Cummings [18].

A major head protein precursor of 32.6 kDa (Figure 5, band A) encoded by ORF150, was substantially smaller than its predicted theoretical size of 50.6 kDa. The mass spectrometry was able to recover 15 peptides located near the C-terminus of the protein precursor, accounting for 44% of the overall amino acid sequence (Table S2). This observation suggests that a truncated form of the mature head protein likely arose as a result of proteolytic cleavage at the N-terminus during head morphogenesis of AKFV33. Others have similarly observed that post-translational processing of the T5 head protein produces a 32 kDa protein [19].

A pore-forming tail tip protein (pb2; Figure 5, band D) was observed to have a molecular mass of 121.1 kDa, similar to the 123.9±0.1 kDa of Pb2 previously obtained from T5 phage [20]. A larger theoretical molecular weight (132.3 kDa) and no coverage of peptides from Arg (R^{1134}) to C-terminus may indicate that this protein also underwent cleavage during morphogenesis [19]. Similarly, Boulanger et al. [20] observed that maturation of Pb2 occurred from the C-terminal end with cleavage after Val^{1148}. In addition, ORF142 possessed identical amino acid sequences at both the N-terminus and C-terminus to that of Pb2 in phage T5 (Figure
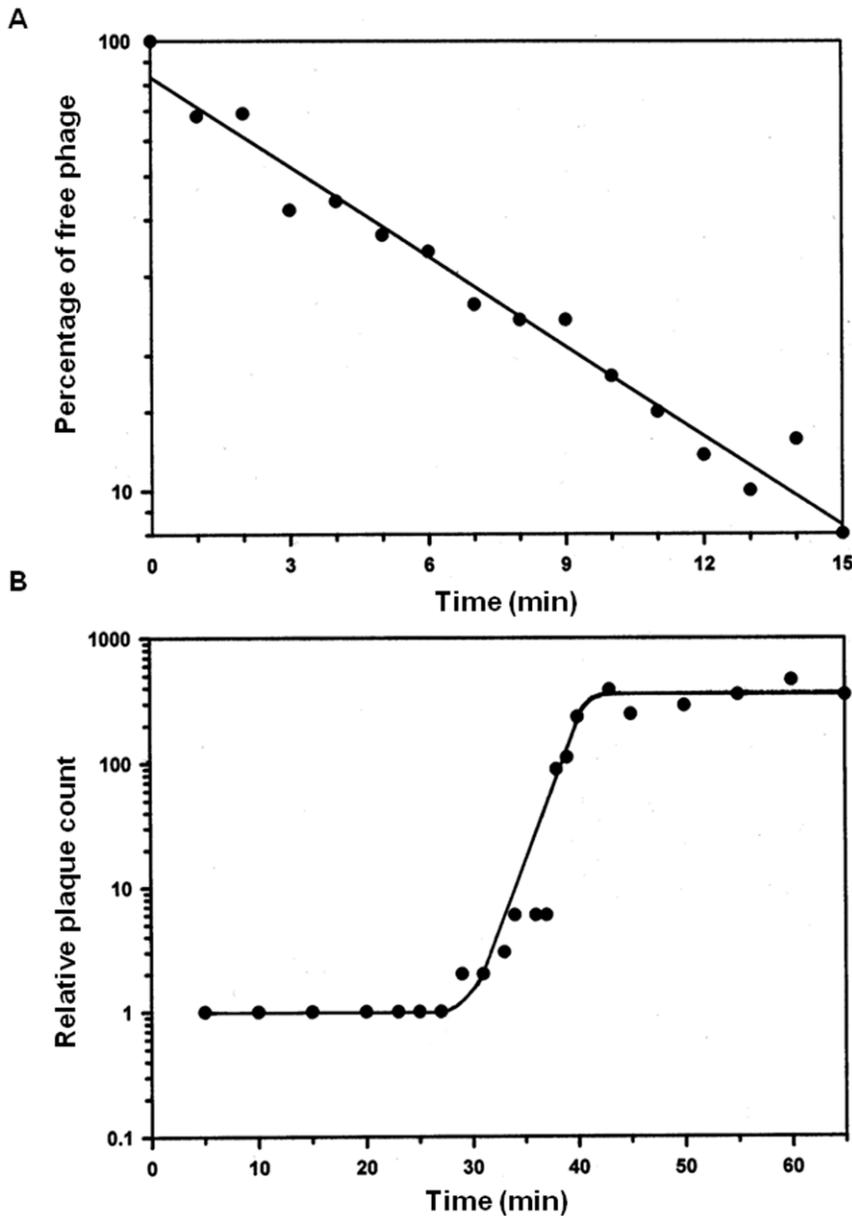
Figure 2. Growth parameters of AKFV33. A, Adsorption curve; B, One step growth curve. Each curve was generated by averaging results from three independent measurements.
doi:10.1371/journal.pone.0034585.g002

S5), despite these proteins only exhibiting an overall sequence identity of 59%. The secondary protein structure of Pb2 from AKFV33 was predicted to be similar to that of phage T5. Firstly, region I (residues 1–1045) contained 7 regions of coiled-coil structure with >0.6 probability (residues 18–46, 446–473, 577–606, 678–763, 776–804, 846–903, 1004–1045). Following this coiled-coil region, there were 2 regions (residues 1037–1059 and 1061–1083) that were indicative of helical transmembrane spanning segments as illustrated by SOSUI. Lastly, the C-terminal region was predicted to have a zinc metallopeptidase motif located between residues 1142 to 1164.

Discussion

This study is the first systematic *in-vitro* investigation and evaluation of the eligibility of a T5-like phage for therapeutic application against STEC O157:H7. Morphological, genomic and proteomic analyses indicated that AKFV33 is a T5-like phage belonging to the family *Siphoviridae*, and lacks genes coding for virulence factors and generalized transduction. AKFV33 was active against a broad range of STEC O157:H7, including reference strains of 30 common PTs and 27 bovine field isolates. Yet unlike other STEC O157:H7-infecting phages [14,21,22,23,24], AKFV33 did not target non-O157 E. coli. A relative high specificity for non-target *E. coli* of therapeutic phages is a key factor to determine safe application in the mitigation of STEC O157:H7 (Niu *et al.*, unpublished data). Most importantly, AKFV33 exhibited strong lytic activity against virtually all STEC O157:H7 isolates tested.

General genomic features

The genome of phage AKFV33 displayed a higher degree of identity to genes from T5-like phages encoding for DNA

Table 2. General features of phage AKFV33 genome.

| Feature	Value
Size (bp)..	108,853
Total number of sequences..	3
G+C content (%)...	38.95
A, 29.86; T, 31.20; G, 18.99; C, 19.95	
Total ORFs………………………………………………..	160
Average ORF size (bp)……………………………………	586
% of genome coding for proteins…………………………..	86.11
No. of gene products similar to known proteins, total………….	153
No. of gene products similar to known T5, total……………….	148
No. of conserved hypothetical protein with unknown function…	102
No. of hypothetical protein…………………………………...	7
No. of σ70 promoters………………………………………..	32
No. of rho-independent terminators………………………….	19
No. of tRNAs……………………………………………….	22

doi:10.1371/journal.pone.0034585.t002

replication, metabolism, recombination and repair as compared to those coding for structural function. This confirms that T5 phages conserve those genes involved in these cellular functions [25]. However, there are discrepancies among HEs between AKFV33 and T5 phage (ATCC11303-B5). Only two HEs (ORFs 96 and 111) were identified in the AKFV33 genome, compared to the nine predicted in phage T5 (ATCC11303-B5, GenBank accession#: NC_005859). Similarly, a T5-like phage, SPC35 with activity against *Salmonella* and *E. coli* exhibited the highest nucleotide similarity (86%) to AKFV33 and was found to possess genes encoding for two HEs [26], while another T5-like phage EPS7, only possessed a single HE [27]. To date, only three HEs belonging to H-N-H subfamily have been revealed to be located in the tRNA gene region of T5 phage (ATCC11303-B5) [28]. All three of these were not identified in the genome of AKFV33. Moreover, the two HEs of AKFV33 were neither closely related to putative H-N-H-endonuclease P-TflVIII of T5 nor that of the podovirus of *Pseudomonas* phage Φ2. Introns or inteins associated HEs and non-introns/inteins-encoding freestanding HEs are mobile genetic elements that can promote the homing of their own genetic elements into allelic intronless and inteinless sites [29]. Freestanding HEs are more abundant than introns/interns associated HEs in T-even phages [30]. These proteins promote gene duplication and protection of DNA from cleavage, but they
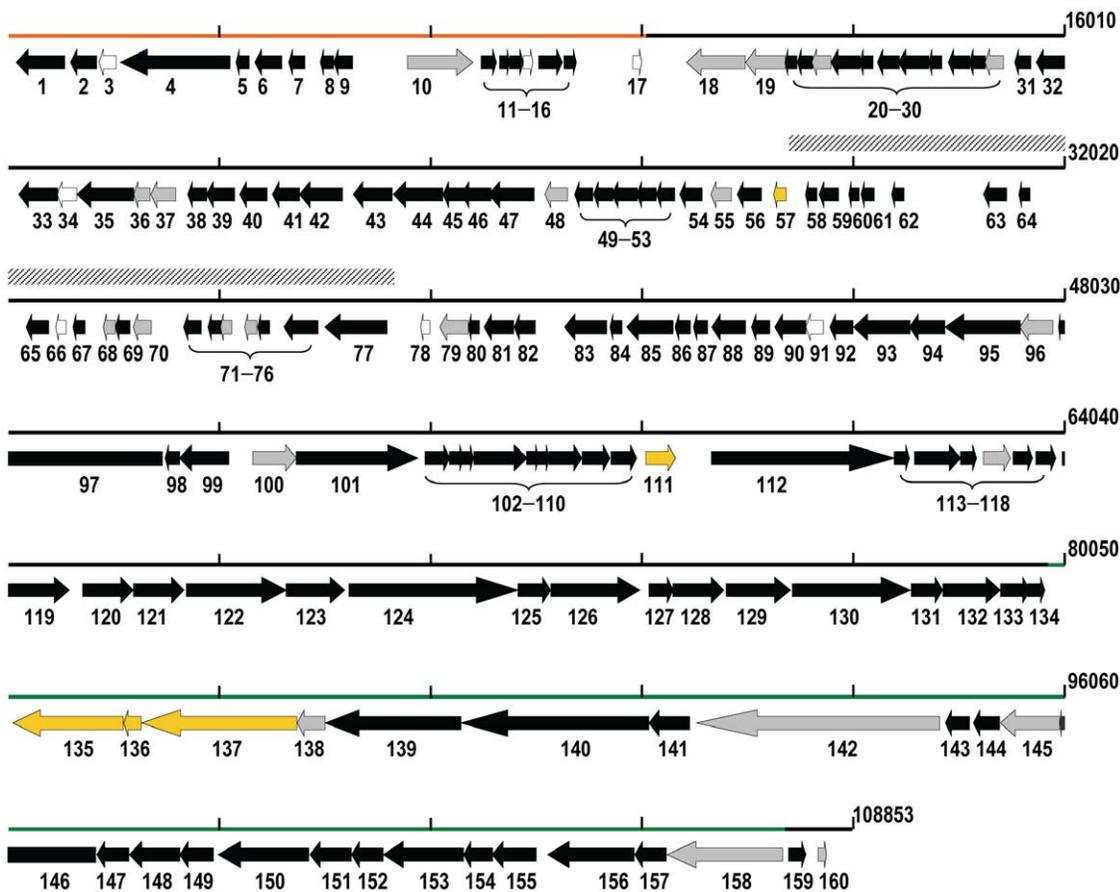
Figure 3. Genomic structure of AKFV33 excluding the terminally redundant DNA sequence. Pre-early, early and late genes regions are indicated by orange, black and green lines, respectively. The predicted ORFs with their directions of transcription are indicated by colored arrows: black, T5-like homologues with greater than 80% identity; gray, T5-like homologues with less than 80% identity; gold, non-T5-like homologues; clear, no homology. The tRNA coding region is indicated by the box with hatched lines.
doi:10.1371/journal.pone.0034585.g003
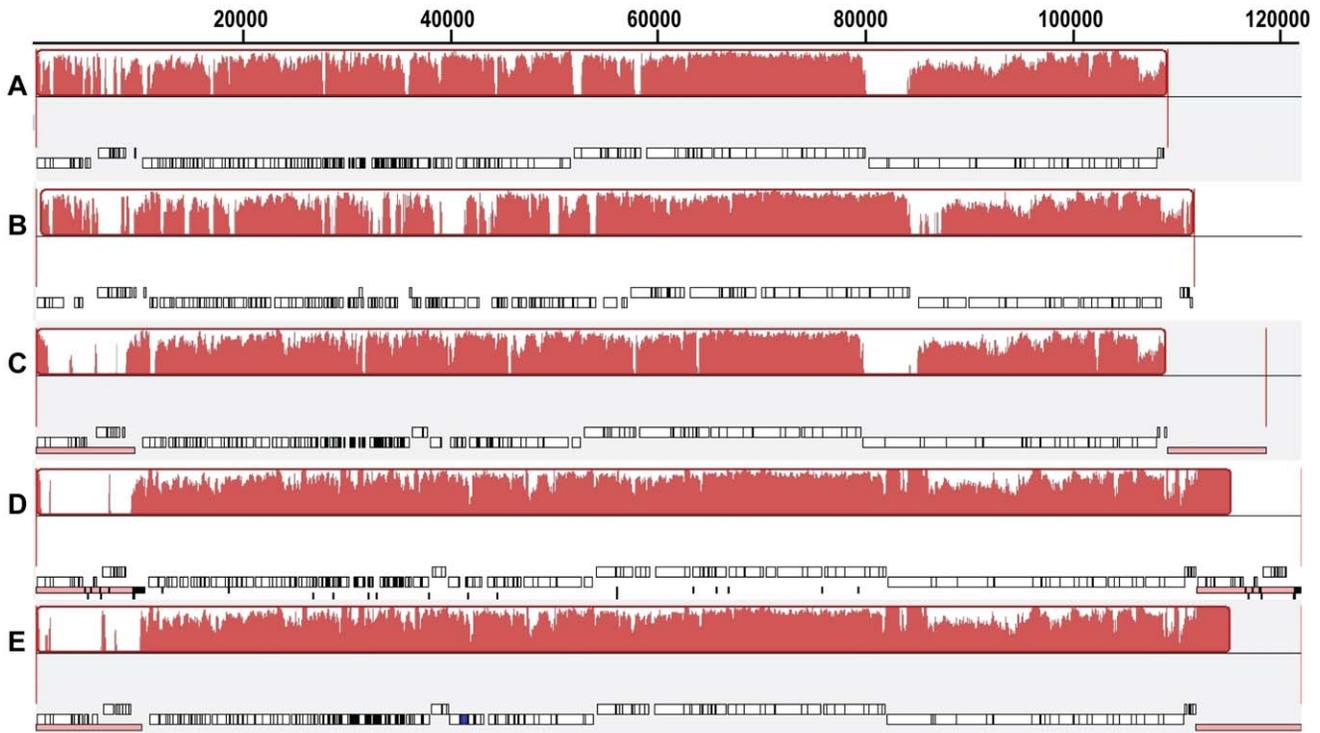
Figure 4. Whole genome comparisons of AKFV33 and other T5-like phages using a progressive MAUVE alignment. The degree of sequence similarity is indicated by the intensity of the red region. The contiguous black boxes under the red region represent the position of the genes. A, AKFV33; B, EPS7; C, SPC35; D, T5 (ATCC11303-B5, GenBank accession#: AY587007); E, T5 (ATCC11303-B5, NC_005859).
doi:10.1371/journal.pone.0034585.g004

are not essential and enter a dynamic cycle of invasion, fixation, inactivation, elimination, and eventually reinvasion [29]. Most HEs have elements that improve gene mobility, maximize insertion site availability, and thereby minimize their probability of being lost from the genome [29]. ORF96 is a counterpart of putative H-N-H-endonuclease P-TflVIII of phage T5 which divides the gene of ribonucleotide reductase into *nrdA* and *nrdB*. Moreover, the *nrdA-nrdB* region appears to be hotspot for HEs insertion in T-even phages, since *mobE*, a freestanding H-N-H endonuclease, has been discovered to lie between the genes of *nrdA* and *nrd*B in several T-even phages [31]. The similar *nrdA-nrdB* splicing H-N-H endonuclease in AKFV33 merits further investigation of its nature and function as it may be similar to *mobE*.

Compared to other T5-like phages, the genome of AKFV33 mainly differed in those structural proteins responsible for host recognition and adhesion. This variation could be responsible for the high specificity of AKFV33 for STEC O157:H7 strains as compared to other T5-like phages [21,25,26,27,32] and non-T5 like STEC O157:H7-infecting phages [14,22,23,24]. Host range is

controlled by the interaction of the phage with receptors on the host cell surface [33]. Host infection and adsorption of phage T5 is initiated by reversible binding of the long tail fibers to the O-antigen of the lipopolysaccharide [34], followed by irreversible binding to outer membrane proteins of FhuA [35] or FepA [32] or BtuB [26] via Pb5. Comparative analysis of the genes and gene products of FhuA, FepA and BtuB using BLASTN and CLUSTALW, respectively, shows that receptor proteins are highly conserved (98–100% identity, BLASTN) among STEC O157:H7 and generic *E. coli*. However, the Pb5 of AKFV33 was not typical of other receptor binding proteins described in T5 phage [25,26,27]. Presumably, the tail fiber protein of this phage was highly specific for the O antigen of STEC O157:H7 isolates, but lacked recognition of O antigen exhibited by the cells of non-O157 *E. coli* strains. Further investigation of host receptors would be required to determine whether co-recognition between tail fiber and Pb5 of this phage occurs when infecting hosts, and if cell surface structures other than FhuA, FepA and BtuB influence recognition and binding of Pb5.

Table 3. Phage AKFV33 structural proteins identified by MALDI QqTOF Mass Spectrometry.

Gel band	ORF	Observed mass (kDa)	Putative function	No. of peptides	Sequence coverage (%)
A	150	32.6	Major head protein	15	44
B	146	51.7	Major tail protein	13	41
C	137	95.8	Tail fiber protein	33	57
D	142	121.1	Pore-forming tail tip protein	23	32

doi:10.1371/journal.pone.0034585.t003
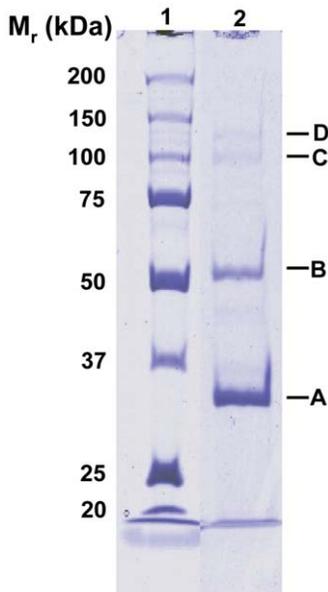
Figure 5. AKFV33 structural proteins (Lane 2) alongside the standard marker (Lane1) separated on 10% SDS-PAGE gel and visualized by Coomassie brilliant blue R250 stain.
doi:10.1371/journal.pone.0034585.g005

Efficacy in biocontrol

To be efficacious, a phage must exhibit high affinity and lytic activity against a variety of strains of the targeted host bacterium. In most cases, failure of phage to attack the host is attributable to a lack of adsorption [33]. Phages with broad spectrum activity against a wide range of STEC O157:H7 isolates could be advantageous in that fewer phages would be required to control this pathogen over a wider range of production environments. Scale-up and production of the phage for commercial applications would also be simplified.

After adsorption, phage DNA must be introduced into the host through the bacterial cell wall [33]. Boulanger *et al.* [20] demonstrated that Pb2 of T5 phage undergoes a conformational change upon binding to the host and possesses fusogenic and muralytic activities that aide in the introduction of DNA into the host. It is probable that the Pb2 of AKFV33 plays a similar role during host infection, as the coiled-coil region of Pb2 could undergo a conformational shift resulting in the formation of a head-tail connector, enabling the C-terminal region to access the host envelope to form a pore in the inner and outer membrane through which phage DNA could be introduced.

Phages with strong lytic capability eliminate pathogens more rapidly and efficiently [36]. Adsorption rate, latent period and burst size are factors that determine the proliferation rate of a given phage [37]. These biological parameters depend on phage type, host physiology and nutritional conditions [33]. Nevertheless, in the present study all STEC O157:H7 screened were highly susceptible [12] to infection by AKFV33. The conserved nature of pre-early region in AKFV33 suggests that it is capable of rapidly shutting off synthesis of STEC O157:H7 DNA, RNA and proteins, degrading host DNA and inactivating host enzymes such as *EcoR*I, *recBC*, DNA methylase and uracil-DNA glycosylase [38]. T5-like phage introduce DNA into their host in a two-step process, with the first step involving the inactivation of host defenses and the second step the replication of phage DNA [38]. The first step involves the introduction of DNA that encodes gene

products such as deoxynucleoside-5′-monophosphatase that ensure deoxynucleotides derived from host DNA are eliminated from the cell prior to the second-step transfer of DNA and the initiation of phage DNA synthesis. Although the mechanisms of two-step DNA transfer in T5-like phages remains unclear, it is imperative that the pre-early mechanisms inactivate host defenses prior to transfer of early and late genes if successful phage replication is to occur [39].

Unlike phages T7 and T4, in which 90% [40,41] and 20% [42,43], respectively, of the deoxynucleotides of the phage DNA are derived from the host DNA, T5 phages do not incorporate nucleotides derived from host DNA into their genome, rather they produce nucleotides almost exclusively by *de novo* synthesis [39]. As a result, T5 is the only T-odd phage identified to date that synthesizes considerably more DNA than is initially present in host at time of infection [39]. Like phage T5, the genome of AKFV33 was found to encode 8 of 11 common enzymes [25] required to generate a pool of nucleotides for DNA synthesis.

T5-like phages contain some of the most efficient promoters characterized and exhibit a high affinity for host RNA polymerase [38]. Phage AKFV33 possessed 32 T5-like promoters plus AT rich regions both around −43 regions around and downstream of +1. Promoters that possess AT-rich regions confer curvature to the DNA strand and increase the stability of the RNA polymerase-promoter complex, thereby increasing transcriptional efficiency [44,45]. Although phages require most of the host's translation apparatus for protein synthesis [46], the overall similar codon usage between AKFV33 and the host would promote efficient translation of gene products [46]. Combined, these properties may contribute to the high transcriptional and translation efficiency and indirectly the high burst size and the low MOI of AKFV33.

As compared to its host STEC O157:H7, the G+C content of AKFV33 was ~11% lower, a difference similar to that reported for other T5-like phages [25,26,27]. Generally, the G+C content tends to be lower in phages than their host due to the reduced availability and higher energetic cost for the synthesis of G and C as compared to A and T/U [47]. Phage DNA typically encodes for tRNAs that when transcribed supplement the host tRNA pools [46]. Presumably, the 22 tRNAs coded for by AKFV33 would compensate for any deficiency of host tRNAs during translation. In phage T5, tRNA genes are expressed from about 5 min after infection until lysis, and are employed in the translation of both early and late transcripts [39].

Safety

As phages are biological entities capable of transferring genetic material among bacterial genomes, safety is major concern for their therapeutic application either on farm or in the food chain. All T5-like phages presently identified are exclusively lytic with none exhibiting lysogenic characteristics [25,26,27,32]. Genomic and proteomic analysis of the genome of AKFV33 identified no sequence that encoded for virulence factors, integration-related proteins or genes coding for antibiotic resistance. As Phage T5 do not utilize host nucleotides for DNA synthesis and the host DNA are degraded and excreted out of the host cell via first-step transfer of DNA [39], the chances of AKFV33 acquiring virulent genes from STEC O157:H7 are remote.

Phage AKFV33 was selected from naturally occurring phages obtained from commercial feedlot cattle. Phage isolates endemic to the environment to which therapy will be applied may result in more efficacious therapeutic outcomes than phage isolated from other environments [21,48]. However, AKFV33 is acid-sensitive a property shared with many other therapeutic phage candidates [49,50,51]. Consequently, the acidic environment of the stomach

may lower phage infectivity [8,9] and acid protection through encapsulation may be necessary for therapeutic application of the phage in livestock.

On-farm strategies of controlling STEC O157:H7 in livestock and their environment have been marginally successful. The present study demonstrates that unique T5-like phage exhibiting specific and high lytic activity against STEC O157:H7 exist within the feedlot environment. Natural fluctuations in STEC O157:H7 populations in the farm environment may be mediated through changes in phage activity. Identification of novel genes that confer a high and specific affinity of T5-like phage for STEC O157:H7 could serve as the foundation for the selection and formulation of phage cocktails to mitigate this pathogen on farm, in the environment and in food.

Materials and Methods

Bacteriophage, bacteria and media

Phage AKFV33 infecting STEC O157:H7 strain R508 (phage type 14, PT14) was isolated from feces from steers housed in a feedlot in 2007 in Alberta, Canada [16]. It was frequently associated with pens of cattle that exhibited reduced prevalence of STEC O157:H7 [16]. A single discrete plaque was purified three times by the soft agar (0.6%) overlay method [52]. Purified phage were then mixed thoroughly with 0.9 ml of sterile lambda diluent (10 mM Tris-HCl, pH 7.5, 8 mM $MgSO_4$) and held at room temperature for 1–2 h to allow phage particles to diffuse from the agar. Diluents containing phage were centrifuged at $10,000 \times g$ for 10 min and filtered through 0.22-µm syringe filter (Pall, Newquay, Cornwall, UK) to remove agar and bacterial cells. The filtrate was used for preparation of working stocks as follows: 100 µl of phage filtrate were mixed with 1 ml of a mid-log-phase culture of STEC O157:H7 strain R508 (OD_{600}: 0.4 to 0.5) and incubated for 15 min at 37°C to enable attachment. This was followed by addition of 250 ml of tryptic soy broth (TSB) amended with $MgSO_4$ at 10 mM, and further incubation at 37°C for 4 to 6 h with shaking (170 rev/min) until complete lysis occurred. The lysates was then centrifuged at $5,250 \times g$ for 20 min at 4°C and filtered through a 0.2-µm SFCA serum filter (Nalgene, Rochester, NY, USA).

Titers of phages in stock filtrates were determined by the soft agar overlay technique [52]. STEC O157:H7 strain R508 was used as a host for plaque purification and titration of phage stocks. Other standard laboratory strains of STEC O157:H7 (n = 36) and non-O157 E. coli (n = 73) [53] used to evaluate host range of AKFV33 are listed in Table 1. Bovine STEC O157:H7 strains (n = 27) endemic to the feedlot pen from which the phage was isolated were grown concurrently with phage AKFV33 as previously described [16]. Unless otherwise indicated strains were grown in TSB and/or tryptic soy agar (TSA).

Host range and lytic capability

Host range and lytic capability of the phage for STEC O157:H7 was assessed using a microplate phage virulence assay [12]. To estimate multiplicity of infection (MOI), high titre phage stocks (10^9–10^{10} PFU/ml) were serially diluted and incubated at 37°C for 5 h with 10-fold diluted overnight cultures of STEC O157:H7 in a 96-well microplate. After incubation, wells were examined visually for turbidity and the highest dilution that resulted in complete lysis (no discernable turbidity) of bacteria was recorded. The MOI for each phage-host assay was calculated by dividing the initial number of phages in the highest-dilution wells by the initial number of bacteria added, as determined by plate counts of the serially diluted bacterial cultures.

Host specificity for seventy-three non-O157 E. coli strains was determined using spot assays. Briefly, each strain of non-O157 E. coli in mid-log-phase (OD_{600}: 0.3 to 0.4) was spread onto modified nutrient agar (MNA) containing NaCl (8.5 g/l), $CaCl_2$ (8.3 mg/l), $FeCl_3$ (1.15 mg/l), $MgSO_4$ $7H_2O$ (0.5 g/l) and 30% (w/v) glucose (10 ml/l) to obtain confluent growth. After the bacterial lawn was dried, 10 µl of phage stock (~10^6 PFU/ml) was spotted on MNA and incubated overnight at 37°C. After incubation, each spot was examined for the presence of clearing zones within the bacterial lawn. Sensitivity of the bacteria to the phage was defined as clearing of >50% of the bacterial spot lawn.

Transmission electron microscopy

Filtered phage lysates (~10^9 PFU/ml) were centrifuged at $25,000 \times g$ for 1 h using an Beckman J2–21 high-speed centrifuge (Palo Alto, CA, USA) and a JA-18.1 fixed angle rotor, followed by two washings in ammonium acetate buffer (0.1 M, pH 7). Phage particles were deposited on copper grids with carbon-coated Formvar films, stained with 2% uranyl acetate (pH 4.5) and examined in a Philips EM 300 electron microscope.

Growth parameters

Phage attachment assays were conducted thrice using the standard method of Kropinski [54] with minor modifications. A mid-log-phase culture of STEC O157:H7 R508 (OD_{600}: 0.3 to 0.4) was mixed with phage lysates to give a MOI of 0.1 and incubated at 37°C. Aliquots (0.2 ml) were taken at 1 min intervals for 15 min and diluted in 19.8 ml of sterile phosphate buffer solution (PBS, pH 7.2, 4°C). The samples were centrifuged at $10,000 \times g$ for 10 min at 4°C and the supernatants were tested for unabsorbed phages through titration using the overlay technique [52]. The adsorption rate constant (k) was calculated.

One-step growth assays were performed thrice using a standard method [37] with modification. A mid-log-phase culture of STEC O157:H7 R508 (OD_{600}: 0.3 to 0.4) was infected by a phage lysates to achieve a MOI of 0.1 and incubated at 37°C for 5 min. The phage-host mixture was centrifuged at $10,000 \times g$ for 10 min at 4°C to remove unabsorbed phages. The pellet containing infected cells was then diluted 1,000- and 20,000-fold, using TSB with 10 mM $MgSO_4$ to a final volume of 10 ml and 20 ml, respectively. The diluted phage-bacteria culture (0.1 ml) was withdrawn immediately to estimate initial phage titre (time zero), and the remainder was incubated at 37°C for one-step growth determination. Samples (0.1 ml) were periodically taken over 60 min, diluted and titrated immediately using the overlay technique [52] and the latent period, the rise period and the burst size was calculated.

pH tolerance assay

Filtered phage lysate (100 µl; ~10^9 PFU/ml) was added to 900 µl of TSB (pH 7.2) and adjusted to a pH of 3.0, 4.5 and 9.3 using either HCl (6 M) or NaOH (6 M) and incubated at 37°C for 16 h. Subsamples (20 µl) were then taken periodically for standard plaque assays [52]. Phage activity was examined in triplicate assays for each pH.

CsCl density gradient centrifugation

Bacterial nucleic acids were removed from filtered phage lysates (~10^9 PFU/ml) using DNase1 (Sigma-Aldrich, Oakville, ON, Canada) and RNaseA (Sigma-Aldrich, Oakville, ON, Canada), and the phage lysates were concentrated in polyethylene glycol (PEG) 8000 and purified through two rounds of CsCl density gradient centrifugation [52].

Genome size estimation

CsCl-purified phages were subjected to pulsed field gel electrophoresis (PFGE) to estimate genome size [55]. Phage DNA embedded in 1% SeaKem Gold agarose (Lonza, Shawinigan, QC, Canada) was subjected to electrophoresis in 0.5×Tris-borate EDTA buffer at 14°C for 18 h using a Chef DR-III Mapper electrophoresis system (Bio-Rad, Mississauga, ON, Canada), with pulse times of 2.2–54.2 s, 6 V/cm. Molecular weight markers were prepared using *Salmonella braenderup* H9812 digested by *Xba*I (Invitrogen, Burlington, ON, Canada). Banding patterns were viewed with UV illumination, and photographed using the Speedlight Platinum Gel Documentation System (BioRad, Mississauga, ON, Canada). All PFGE results were analyzed using BioNumerics software (Applied Maths, Austin, TX, USA).

Genome sequencing and annotation

Phage DNA was extracted from the CsCl-purified phage lysates using the SDS-proteinase K protocol of Sambrook and Russell [52]. Purified phage DNA was submitted to the McGill University and Génome Québec Innovation Centre (Montréal, QC, Canada) and sequenced using 454 Technology by GS FLX Titanium series (Roche Diagnostics, Laval, QC, Canada). The sequence of this phage resided in three large contigs which were closed by PCR.

The genome was initially subjected to automated annotation using AutoFACT [56], with open reading frames (ORFs) subsequently confirmed using Kodon version 2.0 (Applied Maths, Austin, TX, USA). Predicted translated proteins were scanned for homologues using BLASTP and PSI-BLAST [57,58] at http://www.ncbi.nlm.nih.gov. Transfer RNA (tRNA)-encoding genes were screened using Aragorn at http://130.235.46.10/ARAGORN/ [59] and tRNAScan at http://greengene.uml.edu/programs/FindtRNA.html [60]. Rho-independent terminators were identified using MFold [61] and TransTerm [62] at http://nbc11.biologie.uni-kl.de/framed/left/menu/auto/right. Promoters were identified by visual inspection and by a neural network prediction programme at http://www.fruitfly.org/seq_tools/promoter.html. Consensus sequences of the promoters were plotted with WebLogo [63]. Transmembrane domains were described using TMHMM 2.0 at http://www.cbs.dtu.dk/services/TMHMM-2.0/ [64], Phobius at http://phobius.sbc.su.se/ [65], SPLIT 4.0 at http://split.pmfst.hr/split/4/ [66] and SOSUI at http://bp.nuap.nagoya-u.ac.jp/sosui/sosui_submit.html [67]. The COILS program was used to predict coiled-coil structure [68] and PROSITE was used identify conserved motifs [69]. The progressiveMauve algorithm (version 2.3.1) [70] was used to create genome alignment of T5-like phages. CLUSTALW2.1 [71] at (http://www.ebi.ac.uk/Tools/msa/clustalw2/) was used to align amino acid sequences of AKFV33 with other T5-like phages. The nucleotide sequence of the AKFV33 was subsequently deposited with GenBank (Accession #: HQ665011).

Analysis of structural proteins

CsCl-purified phage particles were separated by molecular weight on 10% Sodium dodecyl sulphate-polyacrylamide gel (Bio-Rad Laboratories, Mississauga, ON, Canada). Proteins were stained with Coomassie brilliant blue R250 (Bio-Rad Laboratories, Mississauga, ON, Canada) and subsequently characterized using Bionumerics software (Applied Maths, Austin, TX, USA). Bands of interest were excised, de-stained and dried using a SpeedVac (Savant Instrument, Farmingdale, NY, USA). Following reduction with 10 mM dithiothreitol (DTT) and alkylation with 55 mM iodoacetamide, the protein was digested with 20 ng of sequencing grade trypsin (Roche Diagnostics, Indianapolis, IN, USA) in 25 mM NH_4HCO_3 (pH 7.6) and incubated at 37°C overnight.

The proteolytic peptides were then extracted, and further purified by a C18 Ziptip (Millipore, Billerica, MA, USA). The purified peptides were analyzed by matrix-assisted laser desorption ionization (MALDI) mass spectrometry using an QSTAR XL quadrupole time-of-flight (QqTOF) instrument (AB Sciex, Foster City, CA, USA) under a nitrogen laser (337 nm), with 2,5-dihydroxybenzoic acid as the matrix. Following the MALDI MS analysis, the peptide ions were sequenced by tandem mass spectrometry (MS/MS) using argon as the collision gas. Protein identification was achieved by Mascot (Matrix Science, London, UK) search against the National Centre for Biotechnology Information (NCBI) database, as well as the in-house protein database derived from AKFV33 genome sequences.

Supporting Information

Figure S1 Sequence logos representation of AKFV33 promoters. Consensus sequences were plotted with WebLogo. Height of letter indicates degree of conservation.
(TIF)

Figure S2 Ratio of phage AKFV33 codon usage relative to that of STEC O157:H7 EDL933. The grey bars indicate that codons corresponding to phage-encoded tRNAs.
(TIF)

Figure S3 Sequence comparison from the flap endonuclease (D15) to the conserved hypothetical protein (ORF141) among T5-like phages using a progressiveMAUVE algorithm. The degree of sequence similarity is indicated by the intensity of the red region. The contiguous black boxes under the red region represent the position of the genes and the coloured boxes indicate the conserved genes. Lines link blocks with homology between two genomes. A, AKFV33; B, EPS7; C, H8; D, SPC35; E, T5 (ATCC11303-B5, GenBank Accession#: AY587007).
(TIF)

Figure S4 A, Phylogenetic characterization of the receptor binding protein (*pb5*) of T5-like phages. The sequences were subjected to "one click" phylogenetic analysis incorporating the Gblocks program to eliminate poorly aligned positions and divergent regions at phylogeny.fr [72]. Scale bar represents 0.6 substitutions; B, Amino acid sequence comparison of receptor binding protein (*pb5*) of T5-like phages. The sequence alignment was generated using CLUSTALW2.1. Residues are indicated with an asterisk (*) if identical, a colon (:) if conserved, and a period (.) if related.
(TIF)

Figure S5 Amino acid sequence comparison of poreforming tail tip protein (*pb2*) in phages AKFV33 and T5 (ATCC11303-B5). The sequence alignment was generated using CLUSTALW2.1. Residues are indicated with an asterisk (*) if identical, a colon (:) if conserved, and a period (.) if related.
(TIF)

Table S1 Feature of phage AKFV33 gene products and their functional assignments.
(DOCX)

Table S2 MALDI QqTOF MS and MS/MS analysis of phage AKFV33 structural proteins[a].
(DOCX)

Acknowledgments

Author Contributions

Conceived and designed the experiments: YDN KS TAM. Performed the experiments: YDN HWA RPJ YMS RA. Analyzed the data: YDN AMK AV. Contributed reagents/materials/analysis tools: KS TAM RPJ RA. Wrote the paper: YDN KS AMK HWA RPJ YMS TAM.

References

1. Nyachuba DG (2010) Foodborne illness: is it on the rise? Nutr Rev 68: 257–269.
2. National enteric surveillance program (NESP) annual summary 2009. Public Health Agency of Canada. Available at http://www.nml-lnm.gc.ca/NESP-PNSME/surveillance-2009-eng.html (accessed 25 November 2011).
3. Mohawk KL, O'Brien AD (2011) Mouse models of Escherichia coli O157:H7 infection and Shiga toxin injection. J Biomed Biotechnol 2011: art.no.258185.
4. Callaway TR, Carr MA, Edrington TS, Anderson RC, Nisbet DJ (2009) Diet, Escherichia coli O157:H7, and cattle: a review after 10 years. Curr Issues Mol Biol 11: 67–79.
5. Stephens TP, McAllister TA, Stanford K (2009) Perineal swabs reveal effect of super shedders on the transmission of Escherichia coli O157:H7 in commercial feedlots. J Anim Sci 87: 4151–4160.
6. Karmali MA, Gannon V, Sargeant JM (2010) Verocytotoxin-producing Escherichia coli (VTEC). Vet Microbiol 140: 360–370.
7. Maura D, Debarbieux L (2011) Bacteriophages as twenty-first century antibacterial tools for food and medicine. Appl Microbiol Biotechnol 90: 851–859.
8. Johnson RP, Gyles CL, Huff WE, Ojha S, Huff GR, et al. (2008) Bacteriophages for prophylaxis and therapy in cattle, poultry and pigs. Anim Health Res Rev 9: 201–215.
9. Atterbury RJ (2009) Bacteriophage biocontrol in animals and meat products. Microb Biotechnol 2: 601–612.
10. Balogh B, Jones JB, Iriarte FB, Momol MT (2010) Phage therapy for plant disease control. Curr Pharm Biotechnol 11: 48–57.
11. Rivas L, Coffey B, McAuliffe O, McDonnell MJ, Burgess CM, et al. (2010) In vivo and Ex vivo evaluations of bacteriophages e11/2 and e4/1c for use in the control of Escherichia coli O157:H7. Appl Environ Microbiol 76: 7210–7216.
12. Niu YD, Johnson RP, Xu Y, McAllister TA, Sharma R, et al. (2009) Host range and lytic capability of four bacteriophages against bovine and clinical human isolates of Shiga toxin-producing Escherichia coli O157:H7. J Appl Microbiol 107: 646–656.
13. Anany H, Chen W, Pelton R, Griffiths MW (2011) Biocontrol of Listeria monocytogenes and E. coli O157:H7 in meat using phage immobilized on modified cellulose membranes. Appl Environ Microbiol 77: 6379–6387.
14. Abuladze T, Li M, Menetrez MY, Dean T, Senecal A, et al. (2008) Bacteriophages reduce experimental contamination of hard surfaces, tomato, spinach, broccoli, and ground beef by Escherichia coli O157:H7. Appl Environ Microbiol 74: 6230–6238.
15. Stanford K, McAllister TA, Niu YD, Stephens TP, Mazzocco A, et al. (2010) Oral delivery systems for encapsulated bacteriophages targeted Escherichia coli O157: H7 in feedlot cattle. J Food Prot 73: 1304–1312.
16. Niu YD, McAllister TA, Xu Y, Johnson RP, Stephens TP, et al. (2009) Prevalence and impact of bacteriophages on the presence of Escherichia coli O157:H7 in feedlot cattle and their environment. Appl Environ Microbiol 75: 1271–1278.
17. Wang I-N, Smith DL, Young R (2000) Holins: the protein clocks of bacteriophage infections. Annu Rev Microbiol 54: 799–825.
18. Zweig M, Cummings DJ (1973) Structural proteins of bacteriophage T5. Virology 51: 443–453.
19. Zweig M, Cummings DJ (1973) Cleavage of head and tail proteins during bacteriophage T5 assembly: selective host involvement in the cleavage of a tail protein. J Mol Biol 80: 505–518.
20. Boulanger P, Jacquot P, Plancon L, Chami M, Engel A, et al. (2008) Phage T5 straight tail fiber is a multifunctional protein acting as a tape measure and carrying fusogenic and muralytic activities. J Biol Chem 283: 13556–13564.
21. Raya RR, Oot RA, Moore-Maley B, Wieland S, Callaway TR, et al. (2011) Naturally resident and exogenously applied T4-like and T5-like bacteriophages can reduce Escherichia coli O157:H7 levels in sheep guts. Bacteriophage 1: 15–24.
22. Villegas A, She YM, Kropinski AM, Lingohr EJ, Mazzocco A, et al. (2009) The genome and proteome of a virulent Escherichia coli O157:H7 bacteriophage closely resembling Salmonella phage Felix O1. Virol J 6: 41.
23. Liao WC, Ng WV, Lin IH, Syu WJ, Liu TT, et al. (2011) T4-Like genome organization of the Escherichia coli O157:H7 lytic phage AR1. J Virol 85: 6567–6578.
24. Kutter EM, Skutt-Kakaria K, Blasdel B, El-Shibiny A, Castano A, et al. (2011) Characterization of a ViI-like Phage Specific to Escherichia coli O157:H7. Virol J. 430 p.
25. Wang J, Jiang Y, Vincent M, Sun Y, Yu H, et al. (2005) Complete genome sequence of bacteriophage T5. Virology 332: 45–65.
26. Kim M, Ryu S (2011) Characterization of a T5-like coliphage, SPC35, and differential development of resistance to SPC35 in Salmonella enterica serovar Typhimurium and Escherichia coli. Appl Environ Microbiol 77: 2042–2050.
27. Hong J, Kim KP, Heu S, Lee SJ, Adhya S, et al. (2008) Identification of host receptor and receptor-binding module of a newly sequenced T5-like phage EPS7. FEMS Microbiol Lett 289: 202–209.
28. Akulenko NV, Ivashina TV, Shaloiko LA, Shliapnikov MG, Ksenzenko VN (2004) Novel site-specific endonucleases F-TflI, F-TflII and F-TflIV encoded by the bacteriophage T5. Mol Biol (Mosk) 38: 632–641.
29. Raghavan R, Minnick MF (2009) Group I introns and inteins: Disparate origins but convergent parasitic strategies. J Bacteriol 191: 6193–6202.
30. Edgell DR, Gibb EA, Belfort M (2010) Mobile DNA elements in T4 and related phages. Virol J 7: 290.
31. Friedrich NC, Torrents E, Gibb EA, Sahlin M, Sjöberg BM, et al. (2007) Insertion of a homing endonuclease creates a genes-in-pieces ribonucleotide reductase that retains function. Proc Natl Acad Sci U S A 104: 6176–6181.
32. Rabsch W, Ma L, Wiley G, Najar FZ, Kaserer W, et al. (2007) FepA- and TonB-dependent bacteriophage H8: receptor binding and genomic sequence. J Bacteriol 189: 5658–5674.
33. Weinbauer MG (2004) Ecology of prokaryotic viruses. FEMS Microbiol Rev 28: 127–181.
34. Heller K, Braun V (1982) Polymannose O-antigens of Escherichia coli, the binding sites for the reversible adsorption of bacteriophage T5+ via the L-shaped tail fibers. J Virol 41: 222–227.
35. Letellier L, Boulanger P, Plancon L, Jacquot P, Santamaria M (2004) Main features on tailed phage, host recognition and DNA uptake. Front Biosci 9: 1228–1339.
36. Levin BR, Bull JJ (2004) Population and evolutionary dynamics of phage therapy. Nat Rev Microbiol 2: 166–173.
37. Adams MH (1959) Bacteriophages. OCLC 326505. New York: Interscience.
38. Sayers JR (2006) Bacteriophage T5. In: Calendar R, ed. The bacteriophages. 2nd ed. New York, NY: Oxford University Press. pp 268–276.
39. McCorquodale DJ (1975) The T-odd bacteriophages. CRC Crit Rev Microbiol 4: 101–159.
40. Labaw LW (1953) The origin of phosphorus in the T1, T5, T6, and T7 bacteriophages of Escherichia coli. J Bacteriol 66: 429–436.
41. Tran NQ, Lee SJ, Richardson CC, Tabor S (2010) A novel nucleotide kinase encoded by gene 1.7 of bacteriophage T7. Mol Microbiol 77: 492–504.
42. Warner HR, Hobbs MD (1969) Effect of hydroxyurea on replication of bacteriophage T4 in Escherichia coli. J Virol 3: 331–336.
43. Miller ES, Kutter E, Mosig G, Arisaka F, Kunisawa T, et al. (2003) Bacteriophage T4 genome. Microbiol Mol Biol Rev 67: 86–156.
44. Calistri E, Livi R, Buiatti M (2011) Evolutionary trends of GC/AT distribution patterns in promoters. Mol Phylogenet and Evol 60: 228–235.
45. Tang GQ, Bandwar RP, Patel SS (2005) Extended upstream A-T sequence increases T7 promoter strength. J Biol Chem 280: 40707–40713.
46. Bailly-Bechet M, Vergassola M, Rocha E (2007) Causes for the intriguing presence of tRNAs in phages. Genome Res 17: 1486–1495.
47. Rocha EPC, Danchin A (2002) Base composition bias might result from competition for metabolic resources. Trends Genet 18: 291–294.
48. Callaway TR, Edrington TS, Brabban AD, Anderson RC, Rossman ML, et al. (2008) Bacteriophage isolated from feedlot cattle can reduce Escherichia coli O157:H7 populations in ruminant gastrointestinal tracts. Foodborne Pathog Dis 5: 183–191.
49. Koo J, Marshall DL, DePaola A (2001) Antacid increases survival of Vibrio vulnificus and Vibrio vulnificus phage in a gastrointestinal model. Appl Environ Microbiol 67: 2895–2902.
50. Jamalludeen N, Johnson RP, Shewen PE, Gyles CL (2009) Evaluation of bacteriophages for prevention and treatment of diarrhea due to experimental enterotoxigenic Escherichia coli O149 infection of pigs. Vet Microbiol 136: 135–141.
51. Ma Y, Pacan JC, Wang Q, Xu Y, Huang X, et al. (2008) Microencapsulation of bacteriophage Felix O1 into chitosan-alginate microspheres for oral delivery. Appl Environ Microbiol 74: 4799–4805.
52. Sambrook J, Russell DW (2001) Molecular cloning: a laboratory manual-3rd ed. New York, NY: Cold Spring Laboratory Press, Cold Spring Harbor.
53. Ochman H, Selander RK (1984) Standard reference strains of Escherichia coli from natural populations. J Bacteriol 157: 690–693.
54. Kropinski AM (2009) Measurement of the rate of attachment of bacteriophage to cells. Methods Mol Biol 501: 151–155.
55. Lingohr E, Frost S, Johnson RP (2009) Determination of bacteriophage genome size by pulsed-field gel electrophoresis. Methods Mol Biol 502: 19–25.
56. Koski LB, Gray MW, Lang BF, Burger G (2005) AutoFACT: an automatic functional annotation and classification tool. BMC Bioinformatics 6: 151.
57. Altschul SF, Madden TL, Schaffer AA, Zhang J, Zhang Z, et al. (1997) Gapped BLAST and PSI-BLAST: a new generation of protein database search programs. Nucleic Acids Res 25: 3389–3402.
58. Altschul SF, Gish W, Miller W, Myers EW, Lipman DJ (1990) Basic local alignment search tool. J Mol Biol 215: 403–410.
59. Laslett D, Canback B (2004) ARAGORN, a program to detect tRNA genes and tmRNA genes in nucleotide sequences. Nucleic Acids Res 32: 11–16.

60. Lowe TM, Eddy SR (1997) tRNAscan-SE: a program for improved detection of transfer RNA genes in genomic sequence. Nucleic Acids Res 25: 955–964.

61. Zuker M (2003) Mfold web server for nucleic acid folding and hybridization prediction. Nucleic Acids Res 31: 3406–3415.

62. Jacobs GH, Stockwell PA, Schrieber MJ, Tate WP, Brown CM (2000) Transterm: a database of messenger RNA components and signals. Nucleic Acids Res 28: 293–295.

63. Crooks GE, Hon G, Chandonia JM, Brenner SE (2004) WebLogo: A sequence logo generator. Genome Res 14: 1188–1190.

64. Sonnhammer EL, von Heijne G, Krogh A (1998) A hidden Markov model for predicting transmembrane helices in protein sequences. Proc Int Conf Intell Syst Mol Biol 6: 175–182.

65. Kall L, Krogh A, Sonnhammer EL (2004) A combined transmembrane topology and signal peptide prediction method. J Mol Biol 338: 1027–1036.

66. Juretic D, Zoranic L, Zucic D (2002) Basic charge clusters and predictions of membrane protein topology. J Chem Inf Comput Sci 42: 620–632.

67. Hirokawa T, Boon-Chieng S, Mitaku S (1998) SOSUI: classification and secondary structure prediction system for membrane proteins. Bioinformatics 14: 378–379.

68. Lupas A, Van Dyke M, Stock J (1991) Predicting coiled coils from protein sequences. Science 252: 1162–1164.

69. Hulo N, Bairoch A, Bulliard V, Cerutti L, De Castro E, et al. (2006) The PROSITE database. Nucleic Acids Res 34: D227–230.

70. Darling AE, Mau B, Perna NT (2010) progressiveMauve: Multiple genome alignment with gene gain, loss and rearrangement. PLoS One 5: art.no.e11147.

71. Larkin MA, Blackshields G, Brown NP, Chenna R, McGettigan PA, et al. (2007) Clustal W and Clustal X version 2.0. Bioinformatics 23: 2947–2948.

72. Dereeper A, Guignon V, Blanc G, Audic S, Buffet S, et al. (2008) Phylogeny.fr: robust phylogenetic analysis for the non-specialist. Nucleic Acids Res 36: W465–469.